

The study on behaviour of thin accretion disc affected by Poynting–Robertson effect

Debora Lančová,^{1,a} Pavel Bakala,^{1,4} Kateřina Goluchová,¹
Maurizio Falanga,² Vittorio De Falco,² and Luigi Stella³

¹Institute of Physics and Research Centre for Computational Physics
and Data Processing, Faculty of Philosophy & Science in Opava, Silesian
University in Opava, Bezručovo nám. 13, CZ-746 01 Opava, Czech Republic

²International Space Science Institute, Hallerstrasse 6, 3012 Bern, Switzerland

³INAF – Osservatorio Astronomico di Roma, Via Frascati, 33, Monteporzio Catone,
Rome, I-00040, Italy

⁴M. R. Štefánik Observatory and Planetarium, Sládkovičova 41, 920 01
Hlohovec, Slovak Republic

^adebora.lancova@fpf.slu.cz

ABSTRACT

This study deals with the structure of a thin accretion disc under the influence of radiation pressure and Poynting–Roberson effect. The disc is approximated by inhomogeneous dust consisting of point-like particles in vicinity of a point-like source of radiation. We have developed code *PR Trajectories* which computes trajectories of millions of particles forming an accretion disc and provides a lot of informations about the accretion disc.

Keywords: Dust accretion disc –Radiation –Neutron stars –Black holes

1 INTRODUCTION

In the Low–Mass X–ray binaries (LMXBs) with neutron star or black hole, the luminosity of the central object can have a significant influence on the structure of the accretion disc surrounding the compact object. Despite the radiation pressure we also take into consideration the Poynting–Robertson effect which causes changes of angular momentum of a small particle on an orbit of radiating compact body. The accretion disc approximated by inhomogeneous dust consist of point-like particles is exposed to radiation and we can study the changes of its structure, density and time development. The central body is approximated as a point-like source of radiation and we take into account only the photons emitted in equatorial plane. The influence of the radiation to the motion of particles around a compact object is a well-known problem. Abramowicz et al. (1990) found the stress-energy tensor for a three-dimensional sphere in spherically-symmetric spacetime, the Poynting–Robertson effect has been studied in Stahl et al. (2012). Cases with non-stable luminosity were studied in Stahl et al. (2013) and there are many works on accretion on a luminous

star (Miller and Lamb, 2016; Miller et al., 1996). Our work is based on a work of Bini et al. (2011). In the first section we introduce the geometry of studied settings, the equations of motion and problem of the critical radius. In the next section the motion of single particles under influence of the PR effect is presented. Then we are describing used numerical approach for the dust accretion disc. Finally the results are presented as a set of images of stable solution.

2 POYNTING–ROBERTSON EFFECT IN STRONG GRAVITY

The general relativistic description of Poynting–Robertson effect was published in (Bini et al., 2011) involving non-zero photon momentum. The equations of motion are constructed on the background of Kerr metric defined by space–time element parametrized by the specific angular momentum (spin) a in Boyer–Lindquist coordinates

$$ds^2 = -\left(1 - \frac{2r}{\Sigma}\right) dt^2 - \frac{4ra}{\Sigma} \sin^2 \theta dt d\varphi + \frac{\Sigma}{\Delta} dr^2 + \Sigma d\theta^2 + \left(r^2 + a^2 + \frac{2ra^2 \sin^2 \theta}{\Sigma}\right) \sin^2 \theta d\varphi^2, \quad (1)$$

using geometrized units ($c = G = M = 1$), where $\Sigma \equiv r^2 + a^2 \cos^2 \theta$ and $\Delta \equiv r^2 - 2r + a^2$. We consider the motion of particles only in equatorial plane where $\theta = \frac{\pi}{2}$.

The Kerr metric describing the final state of the gravitational collapse of a massive rotating star into a black hole can also be applied to describe the spacetime in the vicinity of a massive, fast rotating neutron star (Török et al., 2012).

2.1 Radiation field

The central body is approximated by a point-like source of photons. We consider only photons emitted in equatorial plane, the photons angular momentum b is one of the free parameters. (Bini et al., 2011).

The strength of the radiation is represented by constant A which corresponds to the luminosity of central object measured by observer in infinity to the Eddington limit

$$A = \frac{L_{inf}}{L_{Edd}}. \quad (2)$$

The parameters are connected by relation

$$\cos \beta = \frac{bE}{\sqrt{g_{\phi\phi}}E(n)}, \quad (3)$$

where E is a energy of photons and β is azimuthal angle of the photon 4-momentum measured in the local frame related to ZAMO (Zero Angular Momentum Observer) on given radius.

2.2 Equations of motion

We have rewritten the equations of motion published in (Bini et al., 2011) explicitly for the case of the Kerr spacetime as the set of four first-order differential equations. The first pair of equations describes test particle motion in the ZAMO frame by the local spatial velocity v and its azimuthal angle α . The second pair transforms these ZAMO quantities into the radial velocity v_r and the angular velocity ω measured by the static observer at infinity.

$$\begin{aligned}
 \frac{dv}{dt} &= -\sqrt{\frac{\Delta}{g_{\phi\phi}}} \gamma^{-2} \sin \alpha \left(a^{\hat{r}} + 2v \cos \alpha \theta^{\hat{r}}_{\hat{\phi}} \right) \\
 &\quad + \Psi \left[\cos(\alpha - \beta) - v \right] \left[1 - v \cos(\alpha - \beta) \right], \\
 \frac{d\alpha}{dt} &= -\sqrt{\frac{\Delta}{g_{\phi\phi}}} v^{-1} \cos \alpha \left(a^{\hat{r}} + 2v \cos \alpha \theta^{\hat{r}}_{\hat{\phi}} + v^2 k^{\hat{r}}_{(lie)} \right) \\
 &\quad + \Psi \left[v^{-1} - \cos(\alpha - \beta) \right] \sin(\alpha - \beta), \\
 \frac{dr}{dt} &= v^r = \sqrt{\frac{\Sigma}{g_{\phi\phi}}} v \sin \alpha, \\
 \frac{d\phi}{dt} &= \omega = \frac{\sqrt{\Delta}}{g_{\phi\phi}} v \cos \alpha + \Omega_{ZAMO}, \\
 \Psi &= \frac{\lambda \mathcal{L}}{\gamma \sqrt{g_{\theta\theta} g_{\phi\phi}} \cos \beta |\sin \beta|}.
 \end{aligned} \tag{4}$$

where we use quantities expressed with related to free test particle and measured with respect to ZAMO frame (Bini et al., 2011), the Lorentz factor γ corresponds to

$$\gamma = \frac{1}{\sqrt{1 - v^2}}, \tag{5}$$

the radial component of free test particle 4-acceleration $a^{\hat{r}}$, the radial component of shear vector $\Theta_{\hat{\phi}}$ and the radial component of associated Lie relative curvature vector $k^{\hat{r}}_{(lie)}$ are

$$a^{\hat{r}} = \frac{(r^2 + a^2)^2 - 4a^2 r}{r^3 \sqrt{\Delta} g_{\phi\phi}}, \tag{6}$$

$$\Theta_{\hat{\phi}} = -\frac{a(3r^2 + a^2)}{r^3 g_{\phi\phi}}, \tag{7}$$

$$k^{\hat{r}}_{(lie)} = -\frac{\Delta^{-1/2}(r^3 - a^2)}{r^3 g_{\phi\phi}}. \tag{8}$$

2.3 Critical radius

Even from non-relativistic description follows that small particle under influence of Poynting–Robertson effect cannot stay on stable circular orbit and has to either reach the surface of the radiating body or escape to infinity. However, for Schwarzschildcase one can find a radial distance r_{crit} where the radiation pressure and gravitational pull is balanced and particle ends its motion on this critical radius r_{crit} with $v_{crit} = 0$.

However, only in Schwarzschild spacetime (with $a = 0$) one can find the implicitly given value of the r_{crit} (Bini et al., 2009):

$$\frac{A}{MN} = \text{sgn}(\sin\beta_0) \frac{1 - \frac{b^2}{Mr_{crit}} \left(1 - \frac{2M}{r_{crit}}\right)^2}{\left[1 - \frac{b^2}{r_{crit}^2} \left(1 - \frac{2M}{r_{crit}}\right)\right]^{\frac{3}{2}}}. \quad (9)$$

In other settings the r_{crit} can be easily found numerically.

The critical radius goes to infinity with $A = 1$, with low values of A it is very close to the event horizon. In very rare situations there can exist more than one critical radius, for example when the luminosity parameter extends value $A = 0.647$ and the impact parameter $b > 2$. The stability of such state is discussed in (Bini et al., 2009).

3 MOTION OF TEST PARTICLE

The motion of one test particle under the influence of Poynting–Robertson effect has unexpected properties. The particle is spiraling to the inner edge, however the radial component of its 4-velocity has remarkable profile with loops (figure 2). In some cases the radial component of 4-velocity can change the sign during the motion so particles are moving alternately inwards and outwards. At the radii corresponding to loops the particles spends more time. With high value of luminosity the trajectories can be significantly excentric as the radiation pressure pushes the particle far from the central body, yet due to loss of angular momentum the particle falls back.

In the structure of an accretion disc consisting of millions of such particles there are visible peaks of density at radii corresponding to loops in radial component of 4-velocity (figure 1). The structure of the disc is significantly different from structure of accretion disc consisting of particles on almost Keplerian orbits.

4 NUMERICAL IMPLEMENTATION

The numerical model approximates a thin accretion disc by non-interacting particles whose motion is driven by equations 4. The viscosity and scattering of radiation in the disc material are neglected. The inner edge r_{inner} of the disc is set to event horizon, the initial radial coordinate of particles r_0 is one of free parameters. The particles have initial velocity v_0 corresponding to Keplerian circular orbit without influence of radiation v_{kep} which

expressed in ZAMO frame is equal (Bini et al., 2009)

$$\nu_{kep} = \frac{a^2 \mp 2a\sqrt{Mr} + r^2}{\sqrt{\Delta}(a \pm r\sqrt{\frac{r}{M}})}. \quad (10)$$

In some cases we are also simulating small randomization of initial parameters r_0 and ν_0 which are linked by $\frac{\Delta\nu_0}{\nu_0} = \frac{1}{2} \frac{\Delta r_0}{r_0}$.

Because the time scale of one particle falling to the inner edge is very short, the code needs to simulate constant inflow of particles. In every integration step is added a particle on the outer edge of area of interest.

For integration of motion the code using Runge–Kutta method of 8th order. The code is highly parallelised using *OpenMP* library, nevertheless the accretion disc consisting of hundreds thousands particles requires a considerable computational power.

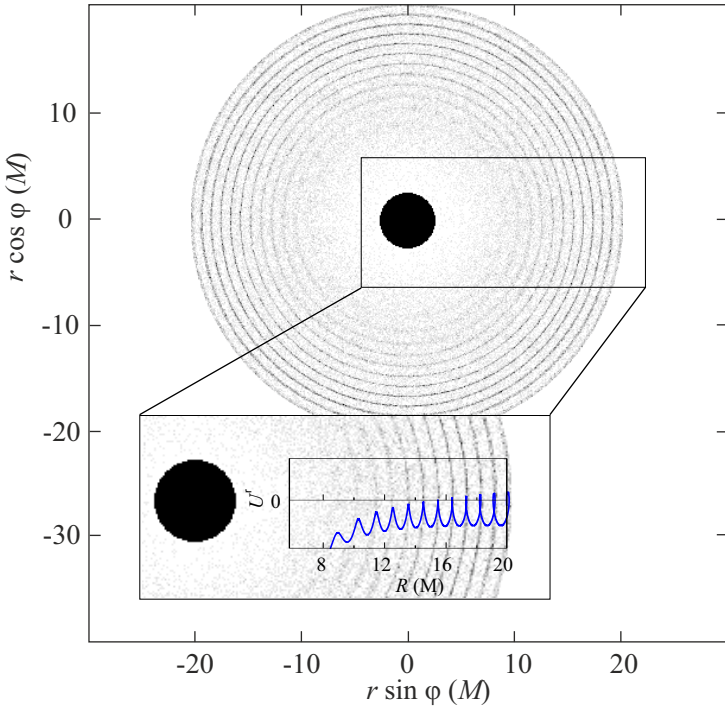


Figure 1. Structure of accretion disc consisting of particles driven by PR effect in comparison with radial component of 4-velocity of single particle. The peaks in density corresponds to the loops in 4-velocity. ($A/M = 0.01$, $a/M = 0.0$, $b/M = 0.0$, $R_0 = 20$ M)

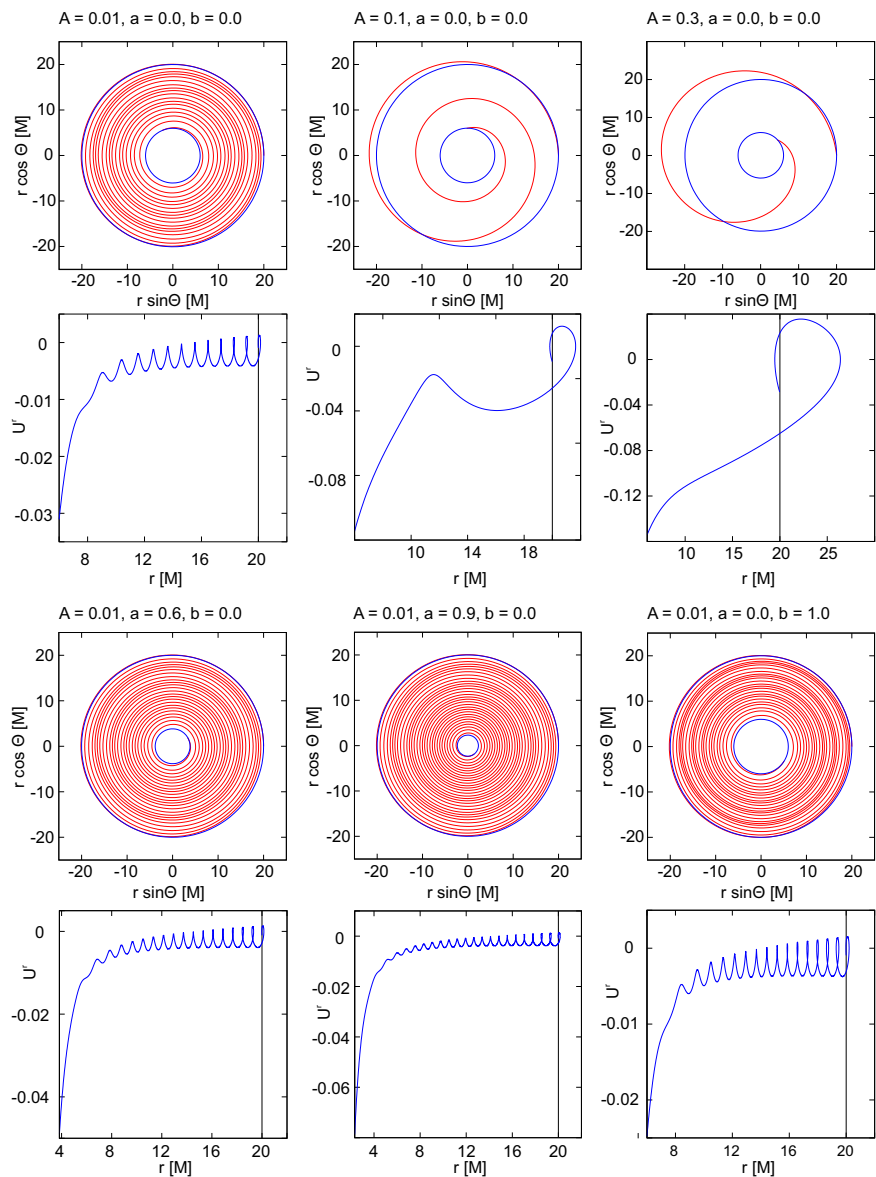


Figure 2. Examples of trajectories of single particle with different initial state and the evolution of its radial component of 4-velocity. The initial radial coordinate is always $r_0 = 20$ M, the inner edge is on innermost stable circular orbit.

5 RESULTS

For study of behaviour of thin accretion disc the simulating code computes trajectories of many particles and in certain times printing their positions in Boyer–Lindquist coordinates. Due to the presence of radiation, distinctive pattern occurs in the structure of the accretion disc. On certain radii is the density of the disc matter is higher causing dark rings to appear. These structure in the disc reflex the changes in radial component of 4-velocity. The number and positions of this rings are very sensitive to initial state of the simulation.

With constant value of luminosity and with constant accretion inflow the disc reaches quasi-stable state although the particles are still rapidly falling to the central body. The distribution of matter in disc is henceforward unchanged.

The structure of the accretion disc depends significantly on the initial condition. Following figures shows selection of simulations result with different values of luminosity A , spin a , radiation field angular momentum b or with slightly scattered initial radial coordinate r_0 or velocity v_0 .

6 CONCLUSION

The results of the simulations shows us significant influence of Poynting–Robertson effect on thin accretion discs. The radiation pressure causes inhomogeneous distribution of matter with significant peaks on certain radii, however the structure strongly depends on the initial parameters of simulation.

In further work we would like to also work on the influence of fast changes of luminosity on the structure of dust accretion disc, e.g. during the thermonuclear X-ray bursting on the surface neutron star.

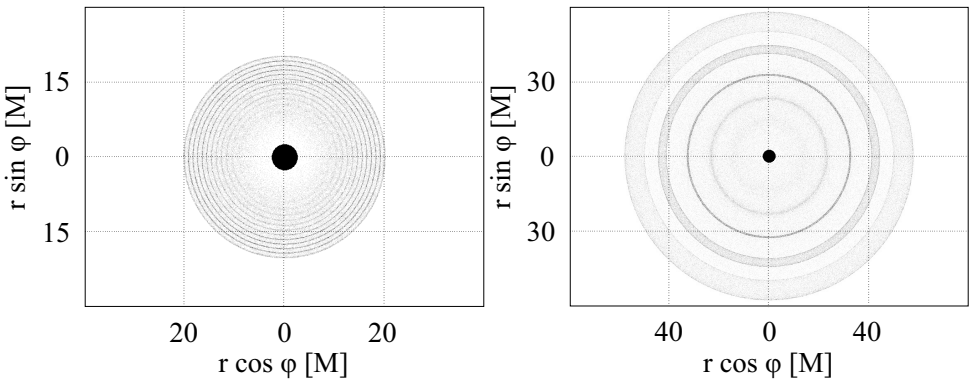


Figure 3. Different luminosities: Left $A/M = 0.01$, $a = 0.0$, $b = 0.0$, $r_0 = 20$ M, $v_0 = v_{kep}$. Right $A/M = 0.1$, $a = 0.0$, $b = 0.0$, $r_0 = 50$ M, $v_0 = v_{kep}$.

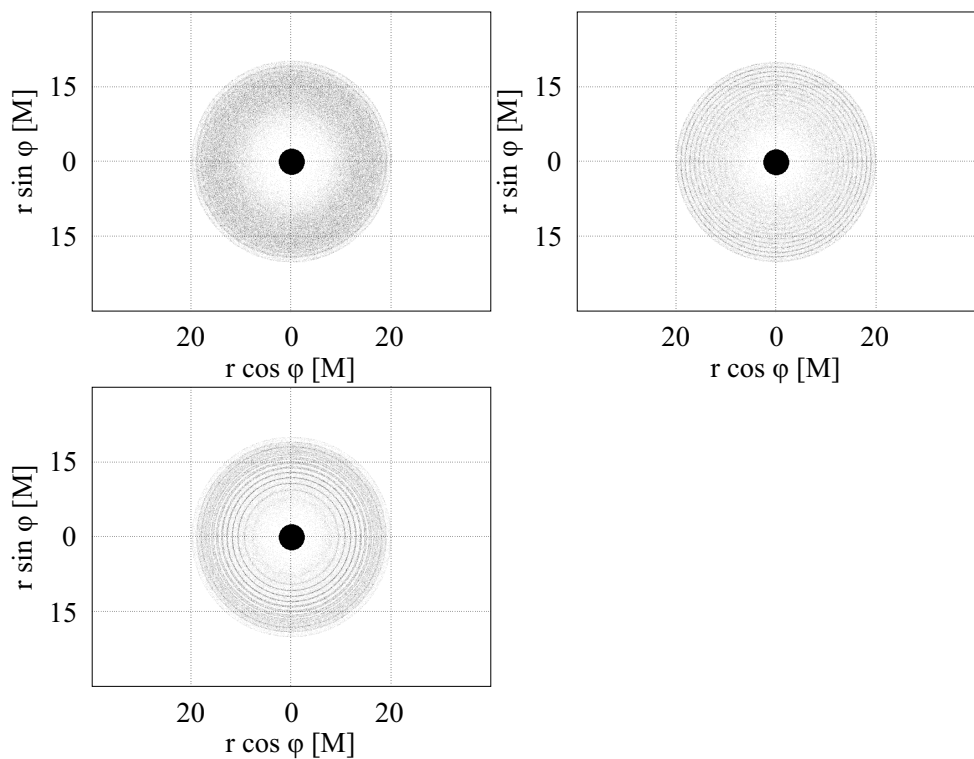


Figure 4. Randomization of initial parameters: $A/M = 0.01$, $a = 0.0$, $b = 0.0$, $r_0 = 20$ M, top left $v_0 = v_{kep} \pm 5\%$, top right $v_0 = v_{kep} \pm 1\%$, bottom $v_0 = v_{kep} \pm 1\%$, $r_0 = 20$ M $\pm 0.5\%$

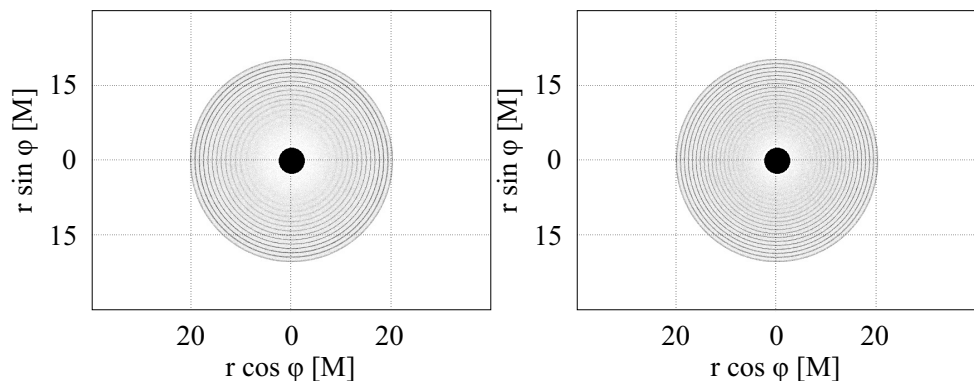


Figure 5. Non-zero spin: $A/M = 0.01$, $b = 0.0$, $r_0 = 20$ M, $v_0 = v_{kep}$, left $a = 0.2$, right $a = 0.6$

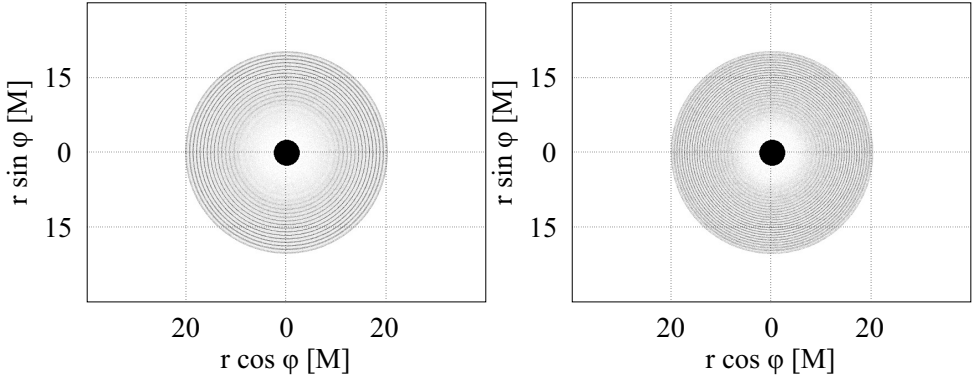


Figure 6. Non-zero radiation field angular momentum: $A/M = 0.01$, $a = 0.0$, $r_0 = 20 M$, $\nu_0 = \nu_{kep}$, left $b = 1.0$, right $b = 2.0$

ACKNOWLEDGEMENTS

We acknowledge the Czech Science Foundation (GAČR) grant No. 17–16287S, the internal grants of Silesian university SU SGS/15/2016 and IGS/1/2017, the inter and the MSK project 03788/2017/RRC. Computational resources were supplied by the Ministry of Education, Youth and Sports of the Czech Republic under the Projects CESNET (Project No. LM2015042) and CERIT-Scientific Cloud (Project No. LM2015085) provided within the program Projects of Large Research, Development and Innovations Infrastructures.

REFERENCES

- Abramowicz, M. A., Ellis, G. F. R. and Lanza, A. (1990), Relativistic effects in superluminal jets and neutron star winds, *The Astrophysical Journal* , **361**, pp. 470–482.
- Bini, D., Geralico, A., Jantzen, R. T., Semerák, O. and Stella, L. (2011), The general relativistic Poynting-Robertson effect: II. A photon flux with nonzero angular momentum, *Classical and Quantum Gravity*, **28**(3), 035008, [arXiv: 1408.4945](#).
- Bini, D., Jantzen, R. T. and Stella, L. (2009), The general relativistic Poynting Robertson effect, *Classical and Quantum Gravity*, **26**(5), 055009, [arXiv: 0808.1083](#).
- Miller, M. C. and Lamb, F. K. (2016), Observational constraints on neutron star masses and radii, *European Physical Journal A*, **52**, 63, [arXiv: 1604.03894](#).
- Miller, M. C., Lamb, F. K. and Psaltis, D. (1996), Sonic-Point Model of Kilohertz QPOs in LMXBs, in *American Astronomical Society Meeting Abstracts*, volume 28 of *Bulletin of the American Astronomical Society*, p. 1329.
- Stahl, A., Kluźniak, W., Wielgus, M. and Abramowicz, M. (2013), Escape, capture, and levitation of matter in Eddington outbursts, *Astronomy and Astrophysics* , **555**, A114, [arXiv: 1306.6556](#).
- Stahl, A., Wielgus, M., Abramowicz, M., Kluźniak, W. and Yu, W. (2012), Eddington capture sphere around luminous stars, *Astronomy and Astrophysics* , **546**, A54, [arXiv: 1208.2231](#).

Török, G., Bakala, P., Šrámková, E., Stuchlík, Z., Urbanec, M. and Goluchová, K. (2012), Mass-Angular-momentum Relations Implied by Models of Twin Peak Quasi-periodic Oscillations, *The Astrophysical Journal* , **760**, 138, [arXiv: 1408.4220](#).